

# Modeling of heat transfer in the cooling wheel in the melt-spinning process

**B. Karpe, B. Kosec\*, M. Bizjak**

Faculty of Natural Sciences and Engineering, University of Ljubljana,  
Aškerčeva cesta 12, Ljubljana, Slovenia

\* Corresponding author: E-mail address: borut.kosec@omm.ntf.uni-lj.si

Received 23.02.2011; published in revised form 01.05.2011

## Manufacturing and processing

### ABSTRACT

**Purpose:** In the case of continuous casting of metal ribbons with the melt-spinning process on the industrial scale, larger quantity of melt could lead to a slow excessive warming of the chilling wheel, which would further lead to solidification of a ribbon at non-uniform conditions and increased wearing of the wheel. Primary goal of our work was to determine to what extent the release of heat during contact of the melt/ribbon on the circumferential surface of the chilling wheel affect its surface temperature rise, and inversely how much elevated temperature of the chill wheel surface affects on metal ribbon cooling rate and its solidification velocity.

**Design/methodology/approach:** On the basis of developed mathematical model, a computer program was made and used for analyses of heat transfer in the melt-spinning process.

**Findings:** The calculations show that contact resistance between metal melt and chilling wheel has a great influence on melt/ribbon cooling and chill wheel heating rate, and must not be neglected in numerical calculations, even if its value is very low. In the case of continuous casting, significant "long term" surface temperature increase may take place, if the wheel is not internally cooled. But inner cooling is effective only if wheel casing thickness is properly chosen.

**Research limitations/implications:** Influence of process parameters and chill wheel cooling mode on cooling and solidifying rate over ribbon thickness are outlined.

**Practical implications:** Directions for the chill wheel cooling system design are indicated.

**Originality/value:** New method for determining contact resistance through variable heat transfer coefficient is introduced which takes into account physical properties of the casting material, process parameters and contact time/length between metal melt/ribbon and substrate and enables cooling rate prediction before the experiment execution. In the case of continuous casting, heat balance of the melt-spinning process is calculated and influence of the chill wheel cooling mode on cooling rate of metallic ribbon is analyzed.

**Keywords:** Modeling; Rapid solidification; Metallic materials; Heat transfer; Heat transfer coefficient

#### Reference to this paper should be given in the following way:

B. Karpe, B. Kosec, M. Bizjak, Modeling of heat transfer in the cooling wheel in the melt-spinning process, Journal of Achievements in Materials and Manufacturing Engineering 46/1 (2011) 88-94.

## 1. Introduction

Single roll melt spinning is the most commonly used process for the production of rapidly solidified thin metal foils or ribbons

with amorphous, microcrystalline or even combined microstructure [1]. Two variants of this process are employed.

Free jet melt spinning, where crucible nozzle is located relatively far away from the wheel and planar flow melt casting, where crucible nozzle is so close to the wheel circumferential

surface, that it constrains the melt puddle. It is proved that small gap between nozzle and the wheel damps perturbations in the melt flow, improves stability of the melt puddle and enables production of wider ribbons [2].

In both types of a process, a molten material is introduced onto a surface of the spinning wheel, where melt puddle is formed (Figure 1 and 2). Material is then dragged out from the puddle by relative motion of the wheel. Usually thin ribbons are produced which can leave the wheel surface in solidified, semi-solidified or fully liquid form, depending on the thermal contact resistance between the melt and substrate, heat transfer in the melt and in the wheel, wetting between melt and wheel material, process parameters, and nucleation and crystal growth characteristics of the particular casting material [3, 4]. With regard to the heat and momentum transport relative efficiency, two mechanisms of ribbon formation are distinguished. Thermal controlled mechanism, where solidification of the ribbon is completed in the puddle and dragged out in already solid form and momentum controlled mechanism, where solidification of the ribbon is delayed for some reason and solidification take place further downstream.

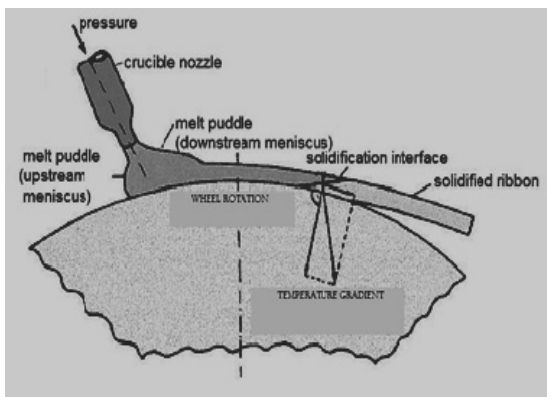


Fig. 1. Scheme of a melt puddle development on the circumferential surface of the wheel at free jet melt-spinning process

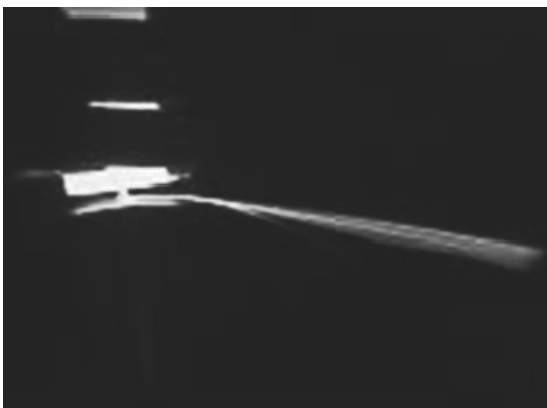


Fig. 2. Snap shot of a melt puddle on the surface of the wheel at free jet melt-spinning process

The most important advantages of rapid solidification, which can be made with this process are extended solubility, refined microstructure, thermal stability at elevated temperatures, and improved magnetic and electrical properties [5, 6].

## 2. Heat transfer calculation

In the case of industrial casting of metal ribbons or foils with the chill block melt spinning processes, like free jet, planar flow or melt extraction, continuous solidification of larger quantities of melt and consecutive heat release could lead to a slow overheating of the chilling wheel [7]. This would further lead to solidification of a ribbon at non-uniform conditions, increased wearing of the wheel or even to the contamination of the casting material with the wheel material. Primary objective of our work was to calculate the temperature field inside the chilling wheel during melt spinning process and to ascertain the influence of the chill wheel surface temperature on metal ribbon cooling rate and solidification velocity [8].

Because melt puddle is thin compared to its width and length we can make an assumption of two-dimensional (2D) transient heat transfer. Assuming 2D transient heat transfer with variable thermal properties and internal heat generation (latent heat of crystallization), general partial differential equation for the melt is reduced to:

$$\frac{1}{r} \cdot (\lambda_m \cdot \frac{\partial T}{\partial r}) + \frac{\partial}{\partial r} \cdot (\lambda_m \cdot \frac{\partial T}{\partial r}) + \frac{1}{r^2} \cdot \frac{\partial}{\partial \varphi} \cdot (\lambda_m \cdot \frac{\partial T}{\partial \varphi}) + \dot{q}''' = \rho_m \cdot c_m \cdot \frac{\partial T}{\partial t} \quad (1)$$

And for chill wheel, where no heat is released by wheel material:

$$\frac{1}{r} \cdot (\lambda_w \cdot \frac{\partial T}{\partial r}) + \frac{\partial}{\partial r} \cdot (\lambda_w \cdot \frac{\partial T}{\partial r}) + \frac{1}{r^2} \cdot \frac{\partial}{\partial \varphi} \cdot (\lambda_w \cdot \frac{\partial T}{\partial \varphi}) = \rho_w \cdot c_w \cdot \frac{\partial T}{\partial t} \quad (2)$$

where:

$r, \varphi, z$  cylindrical coordinate system [m; rad; m]

$T$  temperature [K]

$\rho_m, \rho_w = \rho(T)$  density of the melt and wheel material [kg/m<sup>3</sup>]

$\lambda_m, \lambda_w = \lambda(T)$  thermal conductivity of the melt and wheel material [W/(m·K)]

$c_m, c_w = c(T)$  specific heat of the melt and wheel material [J/(kg·K)]

$\dot{q}'''$  volumetric heat generation rate [W/m<sup>3</sup>]

For calculation of temperature distribution inside the melt puddle and chill wheel, we used explicit finite difference method (FDM) with cylindrical coordinate system. Thermal properties of the melt and wheel material ( $\lambda(T)$ ,  $c(T)$ ) are temperature dependent and are calculated for each iteration step with linear interpolation from tabulated values. Density in solidification interval of the casting material is changing linearly or parabolic, depending on the alloy solidification type (eutectic, dendritic) [9], whereas density of the wheel material is approximated as constant.

In situations where a detailed description of thermal physics is very complicated, such as in melt-spinning process, where heat

transfer between melt and substrate (wheel) is coupled with fluid flow which is further complicated by the presence of solidified region, combined modes of heat exchange are usually taken into account with the overall heat transfer coefficient. This coefficient ( $\alpha$ ) includes conduction and radiation of heat, as well as any convective effects and is defined as the ratio of the heat flux ( $q$ ) from the liquid metal and solid ribbon across the interface with the wheel, to the temperature difference between molten metal or ribbon and the wheel.

Because the temperatures of the casting material and chill wheel are changing along contact length, numerical modelling of the heat transfer with constant heat transfer coefficient and nominal chill wheel temperature is not realistic. Actually, heat transfer coefficient is dependent on many factors which include physical and thermal properties of the melt and chill substrate, fluid velocity, state and geometry of the chill surface and its temperature. Moreover, molten material solidifies and shrinks, which changes the physical contact from liquid/solid to solid/solid or (solid+gas)/solid. Consequently, value of heat transfer coefficient over entire contact length can vary in wide range.

Furthermore, values of the heat transfer coefficient are difficult to measure with confidence. In literature you can find different techniques. From those based on pyrometric, photocalorimetric or wheel surface temperature measurements with embedded thermocouples, to those based on dendritic arm or interlamellar spacing, but none of them can predict the value of the local heat transfer coefficient particularly accurate.

To simplify the mathematical model, we considered number of assumptions. The local heat transfer coefficient  $\alpha(x)$  is calculated with the integral method for liquid metals flow over flat plate. The approximation of the flat plate is reasonable, because of the large aspect ratio between puddle length and radius of the wheel. Another assumption in our model is to consider that there is no velocity gradient in the puddle. This is not completely true in the actual case, but when metallic materials are cast, we believe that velocity gradient can be neglected for thermal field calculation inside the chill wheel. Namely, metal melts have very low Prandtl number and consequently thermal boundary layer much thicker than velocity boundary layer [10]. Ribbon thickness is also found to be approximately proportional to circumferential velocity of the chill wheel ( $u_w^{-1}$ ) and the pressure in the crucible ( $p^{0.5}$ ), as predicted by continuity and Bernoulli equations [11]. Next assumption is that temperature of the melt in the puddle direct under the impinging jet stays equal to casting temperature, because strong turbulences in that region.

The equation for local heat transfer coefficient  $\alpha(x)$  calculation, included in the numerical scheme is:

$$\alpha(x) = \alpha(R, \varphi_j) = \lambda_m \left. \frac{\partial \theta}{\partial y} \right|_{y=0} = \frac{3 \cdot \lambda_m}{2 \delta_t} = \frac{3 \cdot \lambda_m}{2 \cdot \sqrt{8}} \cdot \sqrt{\frac{u_w}{a \cdot x}} \quad (3)$$

where:

- $u_w$  circumferential velocity of the wheel [m/s]
- $\lambda_m$  thermal conductivity of the casting material (temperature dependent) [W/(m·K)]
- $\delta$  thermal boundary layer thickness [m]
- $a$  temperature diffusivity [m<sup>2</sup>/s]
- $x$  distance from the initial contact point to the actual calculation point [m]

### 3. Results and discussion

Figure 3 represents calculated temperature cooling curves in Al ribbon and heating curves for Cu wheel surface, considering different modes of contact resistance: ideal contact, variable contact resistance ( $\alpha(x) = \text{integral method}$ ) and constant contact resistance through entire contact time/length ( $\alpha(x) = 10^6 \text{ W}/(\text{m}^2 \cdot \text{K})$ ). Value for constant average heat transfer coefficient for aluminium reported by other authors, was obtained by subsequent microstructure analyses [11]. Reported contact times are usually calculated from observations of puddle length with the high speed frame camera and lie in the range between 0.2 and 1 millisecond [12] and are dependent on wheel speed, wheel diameter and casting material properties. In our case, selected values for contact time represent limiting values for the analyses propose, and are calculated as a multiplication of iteration step time interval, restricted by the stability criteria of the numerical solution.

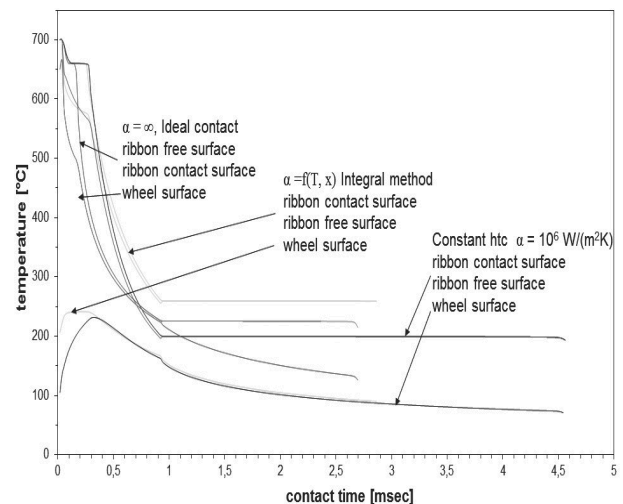


Fig. 3. Cooling curves of free and contact surface of Al ribbon and contact surface of the Cu wheel as a function of different contact resistance. ( $u_w = 18.9 \text{ m/s}$ , ribbon thickness  $66 \mu\text{m}$ , contact time  $0.923 \text{ msec}$ )

Comparison of the contact and free ribbon surface temperature cooling curves, calculated with different approximation of heat transfer coefficient shows, that contact resistance should not be neglected, even if its value is very low. Calculated cooling rate of the melt is relatively much slower when some contact resistance is considered, although its value is very low ( $10^6 \text{ (m}^2 \cdot \text{K)/W}$ ). Integral method calculation of heat transfer coefficient gives the most logical results for entire duration of the contact. Calculated solidification time is practically the same to those obtained by overall heat transfer coefficient, but final temperature of the ribbon at the detachment point is much higher, especially for longer contact time, where constant contact resistance ( $10^6 \text{ (m}^2 \cdot \text{K)/W}$ ) approximation predicts lower ribbon temperature than ideal contact calculation, which is not possible. Cooling of the wheel surface in spite of contact with hotter ribbon seems unlikely, but considering the wheel as a whole, enthalpy of the wheel is increasing, because temperature more than 0.3 mm

under the surface, is increasing entire contact time. Namely, conduction heat transfer rate into the wheel is faster than heat transfer rate across ribbon/wheel interface.

When thicker ribbons are cast or materials with low thermal conductivity, thermal resistance in already solidified region of the ribbon becomes the limiting factor of the heat transfer. High cooling and solidifying rates, through entire cross section of the ribbon, especially on its free surface, can be achieved only when very thin ( $< 30\mu\text{m}$ ) ribbons are cast (Figure 4).

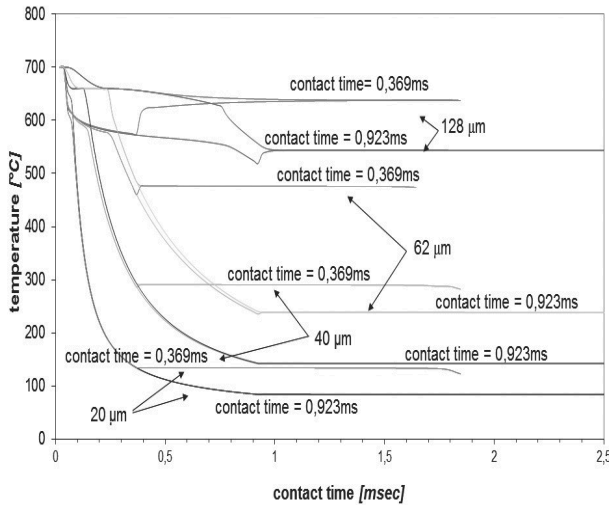


Fig. 4. Calculated cooling curves of contact and free surface of the Al ribbon as a function of its thickness and contact time ( $u_w = 18.9 \text{ m/s}$ ,  $a(x) = \text{integral method}$ )

Wheel material also has significant influence on the cooling rate of the ribbon. Figure 5 shows calculated temperature profiles in steel or copper wheel, when aluminium is cast. As we can see, surface temperature will increase significantly, especially for a wheel of lower thermal diffusivity.

Because short duration of the contact ( $< 1 \text{ ms}$ ) and limited thermal diffusivity of the wheel material, the thermal energy can penetrate only a short distance in the wheel, which results in a higher temperature at the wheel surface. The magnitude of temperature increase depends on the wheel material. For steel wheel, which has much lower thermal diffusivity than copper, an increase of surface temperature is over  $400^\circ\text{C}$ , and heat penetration depth about  $0.5 \text{ mm}$ . On contrary, copper wheel surface temperature increase is about  $200^\circ\text{C}$  and penetration depth twice as much. Of course, when materials with higher melting point are cast, surface temperature of the wheel will increase much higher. Obviously, such a large deviation in surface temperature should not be neglected in calculation of cooling and solidification rate of the melt. Figure 6 shows calculated temperature profiles in aluminium ribbon cast on the circumferential surface of steel or copper wheel as a function of contact time between metal melt/ribbon and surface of the chilling wheel. Importance of wheel material selection is evident. Because contact duration is so short, chilling wheel made from steel is much less effective heat sink than copper wheel and consequently, cooling rate of the ribbon significantly slower.

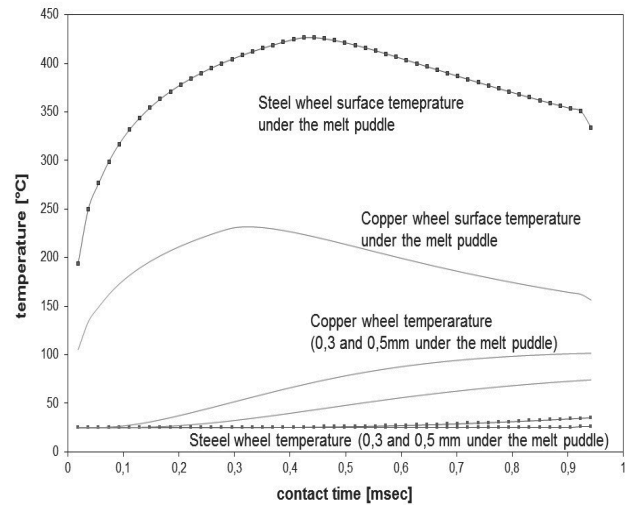


Fig. 5. Steel and copper wheel temperature increase as a function of contact time when aluminium ribbon is cast. ( $u_w = 18.9 \text{ m/s}$ , ribbon thickness  $66 \mu\text{m}$ , contact time  $0.92 \text{ msec}$ ,  $\alpha = 10^6 \text{ W/(m}^2\cdot\text{K)}$ )

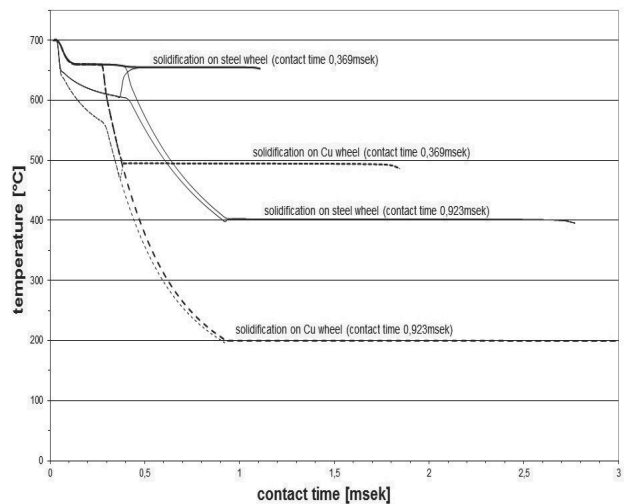


Fig. 6. Calculated cooling curves of Al ribbon as a function of wheel material and contact time ( $u_w = 18.9 \text{ m/s}$ , ribbon thickness  $66 \mu\text{m}$ , contact time  $0.923 \text{ msec}$ ,  $\alpha = 10^6 \text{ W/(m}^2\cdot\text{K)}$ )

During continuous casting process, the wheel is not subjected only to heat transfer from the solidifying material, but also to radiation and convection heat transfer from the crucible. In the case of continuous casting, significant “long term” surface temperature increase may take place, if the wheel is not externally or internally cooled. In calculations discussed above, we have assumed that the wheel surface is at room temperature at the beginning of the contact. For first ten to hundred revolutions surface temperature increase may indeed not be significant, but when continuous casting is performed, especially when materials with high melting point are cast, surface temperature of the wheel can increase in such an extent, that formation of the ribbon will be disturbed, because of decreased cooling and solidifying rate in the



melt puddle. Figure 7 shows the effect of the initial wheel temperature on calculated temperature profiles in the Al ribbon. As we can see, initial wheel temperature has substantial influence on ribbon cooling rate especially, if the contact time is short (high wheel speed). Because melt puddle formation is also momentum controlled, changing the cooling rate could alter solidification pattern in the melt puddle and cause its instability.

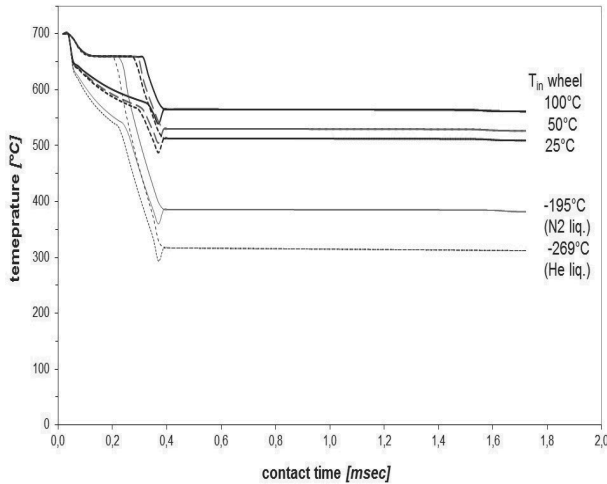


Fig. 7. Cooling curves for 66  $\mu\text{m}$  thick Al ribbon as a function of initial wheel temperature and contact time ( $u_w = 18.9 \text{ m/s}$ , ribbon thickness 66 $\mu\text{m}$ , contact time 0.369msec,  $\alpha(x) = \text{integral method}$ )

Because copper becomes superconductor of heat at cryogenic temperature ( $\lambda_{\text{Cu}} \approx 20000 \text{ W/(mK)}$ ,  $a \approx 20 \text{ m}^2/\text{s}$  at  $T=10 \text{ K}$ ), possibility of liquid gas cooling was analyzed. Calculations, based on the assumption of the same physical contact between the melt and wheel surface, irrespective of the wheel surface temperature indicate that cooling rate will increase substantially for the ribbon of the same thickness. But in spite of much lower wheel surface temperature, the influence of the wheel surface temperature is minor compared to the influence of the ribbon thickness, which mostly depends on the process parameters (Figure 4). Very high cooling and solidification velocities of the melt will still be reached only if the ribbon is thin.

From economical point of view and design simplicity, cooling the wheel with external gas jets or inner rotating water stream is the most promising. For the purpose of the continuous casting on our laboratory apparatus, we calculated temperature heat balance for inner water cooled wheel ( $R_w = 0.2 \text{ m}$ ) as a function of its casing thickness. From the outside, wheel is convectively cooled with surrounding atmosphere, and from the inside with water stream.

In the mathematical model, convective heat transfer coefficients are taken as constants ( $\alpha_{\text{water}} = 5000 \text{ W/(m}^2\cdot\text{K)}$  and  $\alpha_{\text{air}} = 50 \text{ W/(m}^2\cdot\text{K)}$ ) and represent average values, calculated from forced convection correlation equations [9]. No radiation from the crucible is taking into account. To ascertain influence of external cooling with gas jets, we also made calculations, based on assumption of exaggerated value for convective heat transfer coefficient ( $\alpha_{\text{air}} = 1000 \text{ W/(m}^2\cdot\text{K)}$ ), which is practically impossible to attain.

The calculated surface temperatures for 10 mm thick wheel casing are shown in Figure 8. Each saw tooth spike corresponds to the temperature of the wheel surface being underneath the puddle. As we can see, internally water cooled wheel will reach the periodic steady state after few revolutions. But still, long term surface temperature can increase significantly when iron is cast ( $>200 \text{ }^\circ\text{C}$ ), although we assume exaggerated value ( $\alpha_{\text{air}} = 1000 \text{ W/(m}^2\cdot\text{K)}$ ) for convective heat transfer coefficient to the surrounding atmosphere. Namely, duration of one revolution of the wheel is so short that external gas convective cooling would have no significant influence on the wheel surface temperature. Conducting of heat into the wheel and cooling of the inner casing surface with water stream is much faster than external convective cooling with surrounding atmosphere or gas jets.

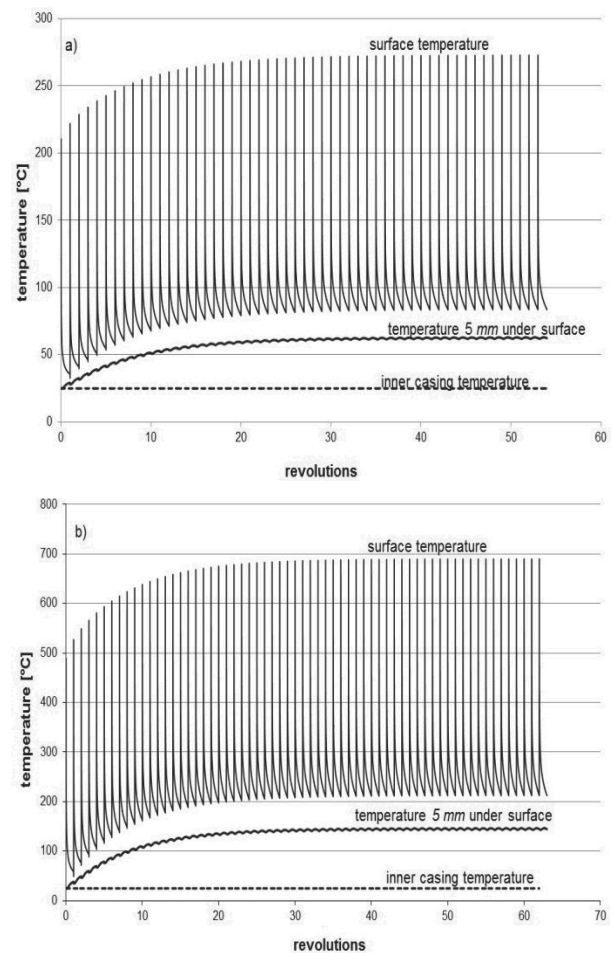


Fig. 8. Surface temperature of the internally water cooled wheel with casing thickness 10 mm and wheel radius 0.2 m a) aluminium casting; b) iron casting ( $u_w = 18.9 \text{ m/s}$ ,  $\alpha_{\text{water}} = 5000 \text{ W/(m}^2\cdot\text{K)}$ ,  $\alpha_{\text{air}} = 50 \text{ W/(m}^2\cdot\text{K)}$ )

If we reduce wheel casing thickness up to 2 mm, internal water cooling will be more effective, and wheel surface temperature that melt will effectively "see" at the beginning of the

next pass of the wheel under the puddle, will be practically the same as at the first revolution, even if high melting temperature materials are cast (Figures 9, 10).

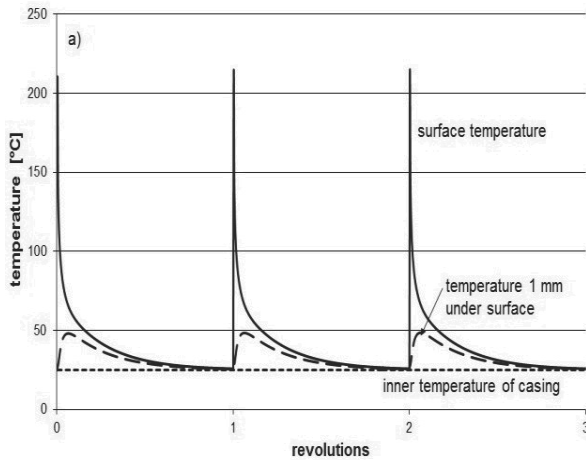


Fig. 9. Surface temperature of the internally water cooled wheel with casing thickness 2 mm and wheel radius 0.2 m, a) aluminium casting ( $u_w = 18.9$  m/s,  $\alpha_{water} = 5000$  W/(m<sup>2</sup>·K) and  $\alpha_{ai} = 50$  W/(m<sup>2</sup>·K))

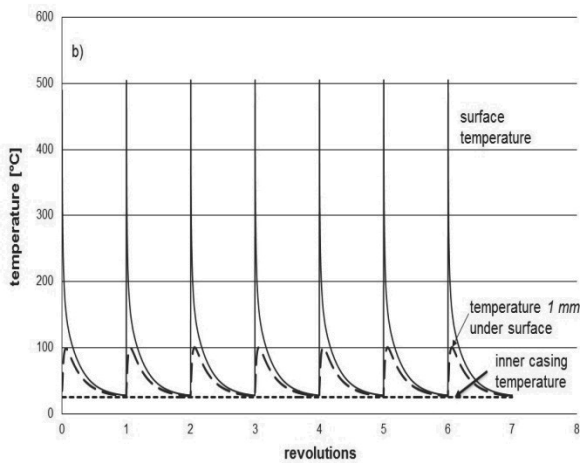


Fig. 10. Surface temperature of the internally water cooled wheel with casing thickness 2 mm and wheel radius 0.2 m, b) iron casting ( $u_w = 18.9$  m/s,  $\alpha_{water} = 5000$  W/(m<sup>2</sup>·K) and  $\alpha_{ai} = 50$  W/(m<sup>2</sup>·K))

But if we reduce wheel casing even further, beneath the heat penetration depth under the melt puddle, convective heat resistance on the inner side (wheel – water interface) becomes significant. Even if we assume heat transfer coefficient value on inner side of a casing as high as 100000 W/(m<sup>2</sup>·K), which can be reached with high pressure impingement water jets [13, 14], heat removal from the melt will be slower as in the case of full or internally water cooled wheel with 10 mm thick casing (Figure 11).

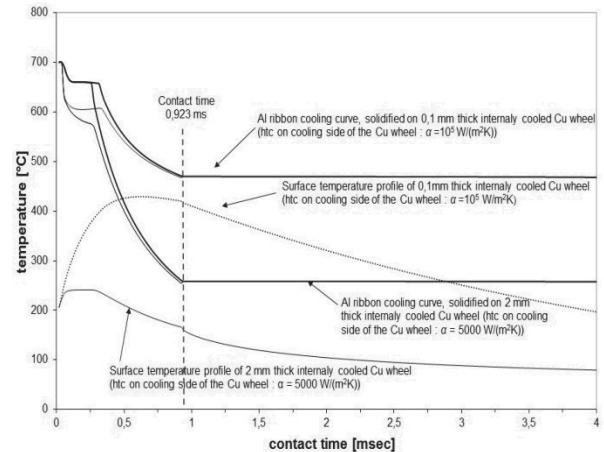


Fig. 11. Internally cooled copper wheel surface temperature increase as a function of contact time and thickness of wheel casing for aluminium casting. ( $R_w = 0.2$  m,  $u_w = 18.9$  m/s, ribbon thickness 66  $\mu$ m, contact time 0.923 msec, hfc on wheel-water side 100000 W/(m<sup>2</sup>·K))

Cooling the thin wheel casing with water stream, flowing between casing and the inner core of the wheel would be even less effective. Because high temperature difference between wheel casing and cooling media, peak heat flux would be exceeded and unstable vapour film formation on inner side of a casing would take place. This phenomenon is called unstable film boiling regime, where heat flux decreases as the surface temperature increases, because the average wetted area of the casing inner surface decrease. Consequently, the wheel casing temperature would increase even more. Reducing the thickness of the wheel casing is unsuitable, from rapid solidification and from steadiness point of view.

## 4. Conclusions

An improved FDM method with variable heat transfer coefficient was used to calculate the heat balance of free jet melt-spinning process.

The mathematical model developed, includes the effect of the conduction heat transfer within the chilling wheel and allows us to investigate the influence of heat contact resistance between the melt and the chill wheel, wheel material, and inner wheel cooling. The fact that the wheel surface temperature is increasing significantly under the solidification melt puddle, selection of the wheel material is important. From rapid solidification point of view, materials with highest temperature diffusivity are preferable. Deoxidized copper has the highest thermal diffusivity between all commercially useful materials, but low mechanical properties at elevated temperature. When wearing of the wheel surface is a problem, Cu-Be or ODS copper alloys are preferable.

For continuous casting internally cooled wheel is preferable, but only in the case when wheel casing thickness is correctly selected. When too thick casing is applied, water cooling will not

have adequate influence on wheel surface temperature increase. When the casing of the wheel is too thin, thermal resistance on the cooling side (wheel-water interface) becomes the limiting factor, which decreases the heat transfer rate from the melt and consequently its cooling and solidifying rate.

## Acknowledgements

The authors want to thank professor Ladislav Kosec (University of Ljubljana) for mentorship at study of rapid solidification and development of advanced shape memory materials, professor Tomaž Kolenko (University of Ljubljana) for information and instructions at computer programming, and professor Mirko Soković (University of Ljubljana) for technical information and discussions.

## References

- [1] M. Bizjak, L. Kosec, A.C. Kneissl, B. Kosec, The characterisation of microstructural changes in rapidly solidified Al-Fe alloys through measurement of their electrical resistance, *International Journal of Materials Research* 99/1 (2008) 101-108.
- [2] B. Kosec, Device for rapid solidifying of metal alloys, *Euroteh* 3 (2004) 32-33.
- [3] T. Haga, K. Inoue, H. Watari, Micro-forming of Al-Si foil, *Journal of Achievements in Materials and Manufacturing Engineering* 40/2 (2010) 115-122.
- [4] L.A. Dobrzański, *Technical and Economical Issues of Materials Selection*, Silesian Technical University, Gliwice, 1997.
- [5] T.J. Praisner, J.S. Chen, A. Tseng, An Experimental Study of Process Behavior in Planar Flow Melt Spinning, *Metallurgical Transactions B* 26 (1995) 1199-1208.
- [6] L.E. Collins, Overview of rapid solidification technology, *Canadian Metallurgy Quarterly* 25/2 (1986) 59-71.
- [7] G. Lojen, I. Anžel, A.C. Kneissl, E. Unterweger, B. Kosec, M. Bizjak, Microstructure of rapidly solidified Cu-Al-Ni shape memory alloy ribbons, *Journal of Materials Processing Technology* 162-163 (2005) 220-229.
- [8] B. Karpe, B. Kosec, T. Kolenko, M. Bizjak, Heat transfer analyses of continuous casting by free jet meltspinning device, *Metallurgy* 50/1 (2011) 13-16.
- [9] D.M. Stefanescu, *Science and Engineering of casting solidification*, Kluwen Academic/Plenum Publishers, Kluwen, 2005.
- [10] J.K. Carpenter, P.H. Steen, On the Heat transfer to the Wheel in Planar – Flow Melt Spinning, *Metallurgical Transactions B* 21/2 (1990) 279-283.
- [11] M.N. Özsisik, *Heat transfer: A Basic Approach*, McGraw-Hill, London, 1985.
- [12] G.X. Wang, E.F. Matthys, Modeling of rapid solidification by melt spinning: effect of heat transfer in the cooling substrate, *Material Science and Engineering A* 136 (1991) 85-97.
- [13] H.H. Libermann, *Rapidly solidified alloys*, Marcel Dekker Inc., London, 1993.
- [14] M. Ciofalo, I. Di Piazza, V. Brucatto, Investigation of the cooling of hot walls by liquid water sprays, *International Journal of Heat and Mass Transfer* 42 (1999) 1157-1175.